

Article

# Poly-(3-ethyl-3-hydroxymethyl)oxetanes—Synthesis and Adhesive Interactions with Polar Substrates

Paweł Parzuchowski <sup>1</sup>  and Mariusz Ł. Mamiński <sup>2,\*</sup> 

<sup>1</sup> Faculty of Chemistry, Warsaw University of Technology, 3 Noakowskiego St., 00-664 Warsaw, Poland; pparzuch@ch.pw.edu.pl

<sup>2</sup> Institute of Wood Science and Furniture, Warsaw University of Life Sciences—SGGW, 159 Nowoursynowska St., 02-776 Warsaw, Poland

\* Correspondence: mariusz\_maminski@sggw.pl; Tel.: +48-22-593-8527

Received: 23 December 2019; Accepted: 14 January 2020; Published: 16 January 2020



**Abstract:** Hyperbranched polyoxetanes are a relatively new class of polymers. These are branched polyethers that are synthesized from oxetanes—four-member cyclic ethers bearing hydroxymethyl groups—via ring-opening polymerization. Four series of polyoxetanes were synthesized from 3-ethyl-3-(hydroxymethyl)oxetane and 1,1,1-tris(hydroxymethyl)propane as a core molecule. Reagents ratios ranged from 1:5 to 1:50, theoretical molar mass ranged from 714 g/mol to 5942 g/mol, and dispersities ranged from 1.77 to 3.75. The morphology of the macromolecules was investigated by a matrix-assisted laser desorption/ionization time of flight technique. The polyoxetanes' adhesive interactions with polar materials were analyzed and provided results as follows: the work of adhesion was 101–105 mJ/m<sup>2</sup>, the bond-line tensile shear strengths were 0.39–1.32 MPa, and there was a brittle fracture mode within the polymer. The findings confirmed a good adhesion to polar substrates, but further research on polyoxetane modifications toward a reduction of brittleness is necessary.

**Keywords:** polyoxetanes; adhesion; hot melt adhesive

## 1. Introduction

Hyperbranched polyoxetanes (POXs) are a relatively new class of polymers. The first syntheses were independently reported by Hult's and Penczek's groups in 1999 [1,2]. However, co-polymerizations of monomers with both oxetanyl and styryl groups were already reported by Motoi et al. in 1989 [3]. POXs are classified as branched polyethers and are synthesized from oxetanes—four-member cyclic ethers bearing hydroxymethyl groups. In the literature, most reports are focused on the polymerization or co-polymerization of 3-ethyl-3-(hydroxymethyl)oxetane (EHO) [4–14]. The monomer for this process is easily available from trimethylolpropane. The main synthetic approach to polyoxetanes goes via cationic ring-opening polymerization, as an anionic mechanism was found to be less effective due to either a low molar mass (ca. 500 g/mol) or broad dispersities ( $M_w/M_n = 4.0\text{--}5.5$ ) and a low degree of branching of the products [15,16]. Investigations on the mechanisms of polymerizations revealed that they undergo an active chain end mechanism (ACE) or an activated monomer mechanism (AMM) [17]. The ACE mechanism is more efficient, as cyclization reactions do not occur.

Polyoxetanes are not paid sufficient attention, though their chemical properties like the ease of side chain functionalization or grafting make them versatile and valuable scaffolds in many fields of material science. Reports on the applicability of functionalized polyoxetanes cover, among others, liquid crystals [18], polymer electrolytes with lithium ion coordination abilities [19,20], fluorine-containing hydrophobic materials [21], amphiphilic block copolymers with poly(ethylene oxide) [22], hybrid networks of fluorine-bearing polyoxetane and inorganic phases [23], hybrid

fluorine-polyoxetane-polyurethane coatings [24], and hyperbranched polyoxetanes in drug delivery systems [25–27]. Wynne and co-workers also used functionalized polyoxetanes to incorporate telechelics in polyurethanes [28,29].

As the number of papers on polyoxetanes is relatively low, the number of works on the adhesive properties of POXs is even lower. Hardly any reports on polyoxetane-based adhesives can be found in the literature.

Jia et al. described a catechol-containing polyoxetane as a platform for an adhesive curable with  $\text{FeCl}_3$  [30]. The investigated adhesives exhibited relatively good strengths on such substrates like metals (3.7–4.9 MPa), poplar wood (2.7 MPa), and glass (2.10 MPa). Further research in that group demonstrated that merging catechol with phosphoric acid and a POX backbone might induce adhesion in humid environments, which may give way to the design of biomimetic adhesives [31]. Reports on photocurable adhesive systems based on epoxides and oxetanes can be also found in the literature [32,33].

In 2016, we made a patent application on the use of poly(hydroxy)oxetanes as hot-melt adhesives in wood bonding [34]. This study presents the synthesis and molecular characteristics of poly-(3-ethyl-3-hydroxymethyl)oxetanes of different molar masses and their adhesive interactions with polar substrates. According to our best knowledge, the present study is the first to discuss POX–lignocellulosic adhesive interactions.

In our approach, POXs were synthesized from 3-ethyl-3-(hydroxymethyl)oxetane by using 1,1,1-tris(hydroxymethyl)propane (TMP) as a core molecule. Such protocol allows for the yield of polymers of a lower dispersity when compared to homopolymerization and easier molar mass control [35].

## 2. Materials and Methods

All chemicals were purchased from Sigma-Aldrich (Poznań, Poland) and used as received; 3-ethyl-3-(hydroxymethyl)oxetane (EHO) was purchased from TCI Europe N.V., (Zwijndrecht, The Netherlands), and used as obtained. Solvents were distilled prior to use.

### 2.1. NMR and FTIR Measurements

$^1\text{H}$  and  $^{13}\text{C}$  NMR spectra were recorded on a Varian Mercury VXR 400 MHz (Agilent Technologies, Santa Clara, CA, USA) NMR spectrometer and used tetramethylsilane as an internal standard in  $\text{DMSO-d}_6$ . FTIR spectra were recorded on a Nicolet iS5 (Thermo Fisher Scientific, Inc., Waltham, MA, USA) spectrometer in attenuated total reflectance (ATR) mode. The measurements were performed in the  $400\text{--}4000\text{ cm}^{-1}$  range with a resolution of  $2\text{ cm}^{-1}$ .

### 2.2. Gel Permeation Chromatography (GPC)

The molar mass and molar mass distribution of the samples of polymers were performed via gel permeation chromatography (GPC) on a Viscotek (Malvern Panalytical Ltd., Malvern, UK) system comprising a GPCmax and a triple detector array (TDA) 305 unit equipped with one guard and two divinylbenzene (DVB) Jordi (JordiLabs LLC., Mansfield, MA, USA) gel columns (102–107; linear; mix bed) in methylene chloride as an eluent at  $35\text{ }^\circ\text{C}$  at a flow rate of  $1.0\text{ mL/min}$  while using a refractive index (RI) detector and polystyrene calibration.

### 2.3. MALDI-TOF Spectrometry

The structure and morphology of the poly(hydroxy)oxetanes were confirmed in MALDI-TOF experiments. Spectra were measured on a Bruker UltrafleXtreme<sup>TM</sup> (Bremen, Germany) instrument and used DCTB (trans-2-[3-(4-tert-butylphenyl)-2-methyl-2-propenylidene]malononitrile) as a matrix. Samples were dissolved in THF.

#### 2.4. Lap Shear Strength

A 0.5 mm thick foil of a POX was applied between two 1.5 mm-thick birch veneers (120 × 20 mm) onto an overlapping area of dimensions 20 × 20 mm and bonded in a hot press at 150 °C for 30 s under 0.8 MPa pressure before immediately being transferred to a cold press and kept 5 min under 0.8 MPa pressure to cool down and set the bond-line. Bonded specimens were conditioned at normal conditions (20 ± 2 °C and 65 ± 5% relative humidity) for 24 h before testing (Instron 3369 universal testing machine; Instron Corp., Norwood, MA, USA). Twelve specimens were tested in each series.

Shear strength ( $R_t$ ) was calculated from the Equation (1):

$$R_t = \frac{F_{\max}}{S} \quad (1)$$

where  $F_{\max}$  is the maximum force in Newtons and  $s$  is lap area in mm<sup>2</sup>.

#### 2.5. Contact Angle ( $\theta$ ) and Work of Adhesion ( $W_a$ )

Wetting experiments were performed on a Phoenix 300 contact angle analyzer (Surface Electro Optics, Suwon City, Korea). Distilled water and diiodomethane were used as the reference liquids. The contact angles measurements were done 30 s after droplet deposition. Calculations of surface free energy were based on the Owens–Wendt method [36]. The work of adhesion between water and POX films was calculated from the Equation (2) [36]:

$$W_a = \gamma_S + \gamma_L - \gamma_{SL} \quad (2)$$

where  $\gamma_S$  is the surface energy of solid,  $\gamma_L$  is the surface tension of liquid, and  $\gamma_{SL}$  is the interfacial tension between a solid and a liquid (Equation (3)):

$$\gamma_{SL} = \gamma_S + \gamma_L - 2\sqrt{\gamma_S^D \gamma_L^D} - 2\sqrt{\gamma_S^P \gamma_L^P} \quad (3)$$

where  $D$  and  $P$  denote the dispersive and polar parts of the free surface energy, respectively. Values for reference liquids were given elsewhere [37].

#### 2.6. Synthetic Procedures

Cationic polymerization of 3-ethyl-3-(hydroxymethyl)oxetane (EHO) with 1,1,1-tris(hydroxymethyl)propane (TMP):

The poly(hydroxy)oxetanes (POXs) were prepared according to the following procedure: in a 250 mL three-neck flask equipped with a magnetic stirrer, thermometer, a rubber septum, a funnel, a nitrogen inlet and a bubble meter, 300 mL of dichloromethane and 2.36 g (17.62 mmol) of TMP were placed. The reaction vessel was degassed by using nitrogen for 20 min, and then boron trifluoride diethyl etherate  $\text{BF}_3\text{Et}_2\text{O}$  (0.13 g, 0.92 mmol) was added via syringe and heated to 70 °C. Then, 10.25 g (88.36 mmol) of EHO was added dropwise at a rate of 5 mL/h. After 2 h at 70 °C, the reaction was quenched with ethanol. The product was precipitated in cold diethyl ether and dried under vacuum.

POXs of various TMP/EHO ratios, as well as a POX without TMP core, were prepared according to the same procedure. Products were obtained with yields ranging between 89% and 95%.

### 3. Results and Discussion

Poly(3-ethyl-3-hydroxymethyloxetane)s can be synthesized according to cationic, anionic or activated monomer mechanisms [1,2,13,15,38,39]. In the case of cationic polymerization, the catalyst concentration and temperature have fundamental impacts on the degree of the branching of the obtained product. Figure 1 shows the mechanism of the reaction and the possible substructures of the polymer. In the structure that was synthesized with the use of trimethylolpropane (TMP) as an

initiator and EHO as a monomer, the starting (S) and terminal (T) units were identical, which simplified the NMR spectra (Figure 2). Other units present in the polymer were dendritic ones (D) in which all hydroxyl groups reacted; linear ones (L), with one free OH group; and terminal cyclic ones (T').

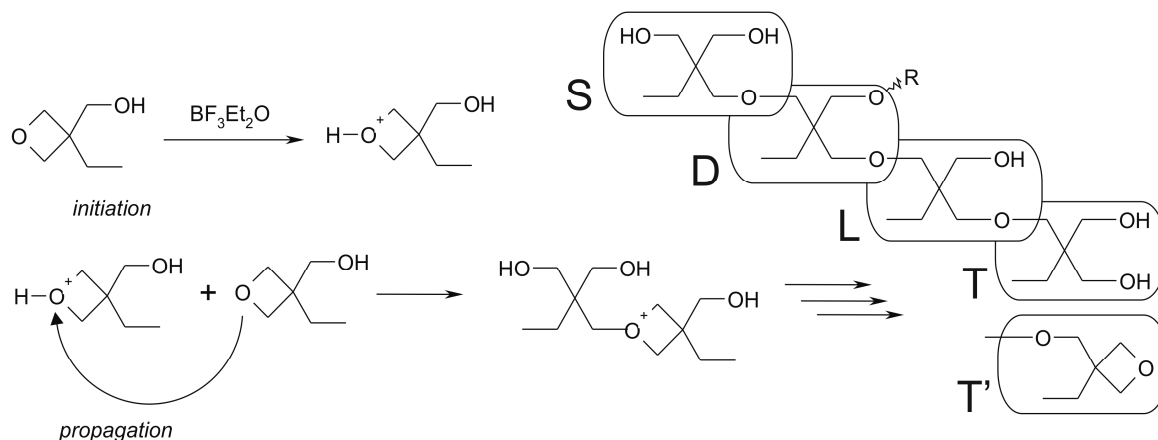


Figure 1. Cationic polymerization of 3-ethyl-3-hydroxymethyloxetane.

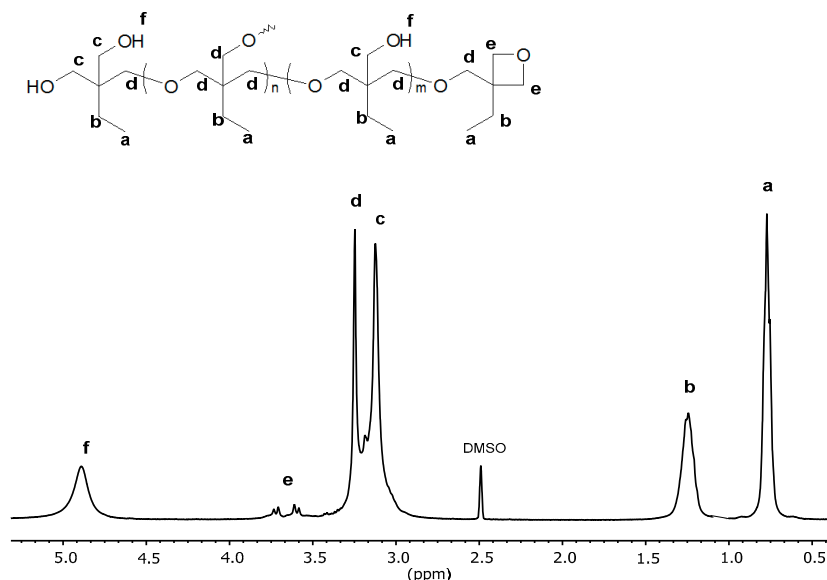


Figure 2.  $^1\text{H}$  NMR (400 MHz,  $\text{DMSO-d}_6$ ) spectrum of poly(3-ethyl-3-hydroxymethyloxetane).

In case of the polymerization of 3-ethyl-3-hydroxymethyloxetane at a constant concentration of catalyst, the number of branching points depended mainly on the reaction temperature. When the reaction was conducted at  $-30$ ,  $-2$ ,  $30$  and  $70$   $^\circ\text{C}$ , the degrees of branching calculated from  $^{13}\text{C}$  NMR spectra by using the Frey equation [38] were equal to 0.21, 0.36, 0.43 and 0.50, respectively.

Figure 2 shows a typical  $^1\text{H}$  NMR spectrum of hyperbranched poly(3-ethyl-3-hydroxymethyloxetane) measured in  $\text{DMSO-d}_6$ . All the signals can be assigned to the structural elements of the polymer:  $-\text{OH}$  (4.7 ppm),  $-\text{CH}_2-\text{O}-(\text{T}')$  (3.7–3.6 ppm),  $-\text{CH}_2-\text{O}-$  (3.3 ppm),  $-\text{CH}_2-\text{OH}$  (3.1 ppm),  $-\text{CH}_2-\text{CH}_3$  (1.3 ppm), and  $-\text{CH}_2-\text{CH}_3$  (0.8 ppm). The doublet of doublets (e) at 3.7 ppm indicates the presence of terminal units  $\text{T}'$  (Figure 1) and was visible only for the polymers synthesized at low temperatures.

The degree of branching of the hyperbranched polyoxetanes was determined with the use of b signals (Figure 3) in the  $^{13}\text{C}$  NMR spectrum. The signal of the methylene group carbon of the ethyl substituent was split according to the chemical surrounding into signals of dendritic ( $\text{b}''$ ), linear ( $\text{b}'$ )

and terminal (b) units. It was deconvoluted and integrated by using MestReNova 10.0.2-15465 software (Mestrelab Research, S.L., Escondido, CA, USA).

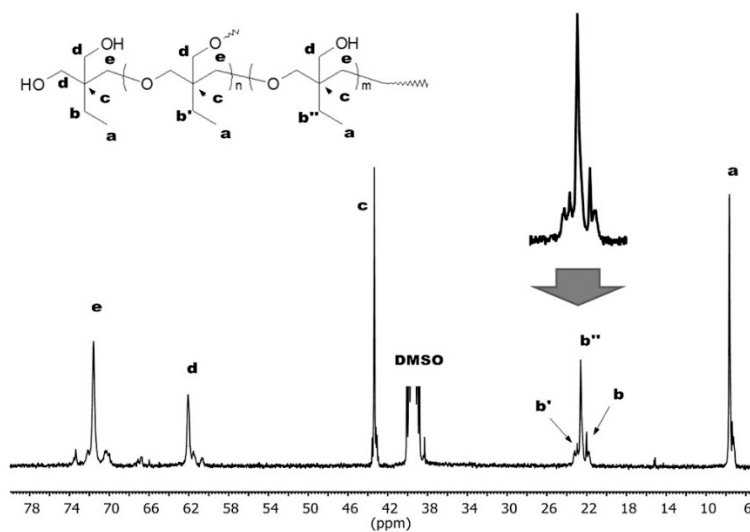


**Figure 3.**  $^{13}\text{C}$  NMR (400 MHz,  $\text{DMSO-d}_6$ ) spectrum of poly(3-ethyl-3-hydroxymethyloxetane) of degree of branching equal to 0.36.

For the purpose of adhesive tests, four polyoxetanes of different molar masses were synthesized. Reagent amounts and theoretical molar masses are shown in Table 1. A high abundance of polar hydroxyl groups is a prerequisite for an adhesive material to form strong interactions with polar substrates. Additionally, thermoplastic character of POXs makes them considered to be potential hot-melt adhesives.

**Table 1.** Molar mass and amounts of reagents used in synthesis of polyoxetanes (POXs).

Theoretical Molar Mass [g/mol]	TMP/EHO Molar Ratio	EHO [g]	TMP [g]	$\text{BF}_3\text{Et}_2\text{O}$ [g]
714	1:5	10.25	2.36	0.13
1295	1:10	18.00	2.36	0.25
2457	1:20	20.50	1.18	0.25
5942	1:50	51.58	1.18	0.63

The reactions were performed at 70 °C to assure high (0.5) degrees of branching and high (>95%) reaction yields. The  $^1\text{H}$  NMR spectra shown in Figure 4 indicate the efficient polymerization of the EHO monomer with the TMP core molecule. The signals of TMP units have the same chemical shifts as signals coming from EHO units which make the spectra quite simple. For the same reason, the calculation of molar mass of the polymers from the NMR spectra was not possible. The T' units signals in these experiments were not visible.

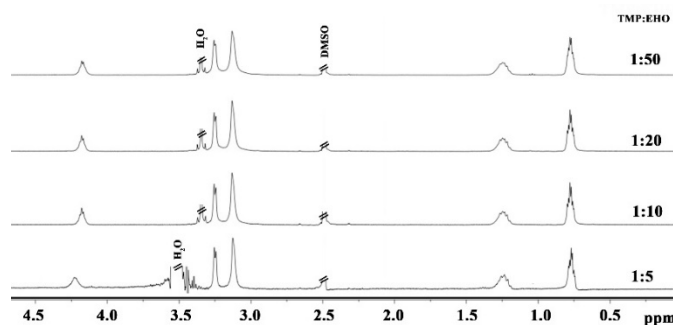


**Figure 4.**  $^1\text{H}$  NMR (400 MHz,  $\text{DMSO-d}_6$ ) spectra of the studied polyoxetanes.

In the FTIR spectra presented in Figure 5, O–H stretch ( $3324\text{ cm}^{-1}$ ),  $\text{CH}_2$  stretch ( $2966\text{ cm}^{-1}$ ,  $2934\text{ cm}^{-1}$  and  $2880\text{ cm}^{-1}$ ) and backbone ether C–O–C stretch ( $1180\text{ cm}^{-1}$  and  $1047\text{ cm}^{-1}$ ) bands are present. It is known that isolated OH groups appear at the ca.  $3600\text{ cm}^{-1}$  wavenumber, whereas hydrogen-bonded hydroxyls appear at lower wavenumbers ( $3400\text{--}3200\text{ cm}^{-1}$ ) [40]. Thus, the band observed at  $3324\text{ cm}^{-1}$  proved the presence of intra- and intermolecular hydrogen bonds within the POXs. Mamiński et al. demonstrated that the partial substitution of hydroxyls in a hyperbranched polymer reduces intramolecular hydrogen-bond formation [41].

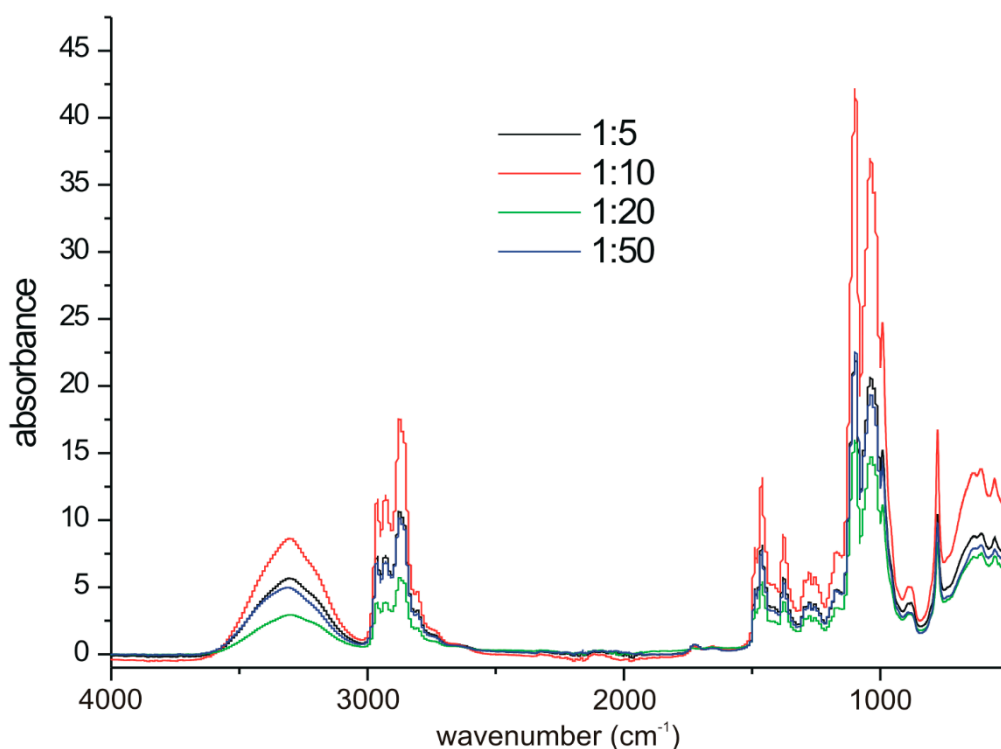


**Figure 5.** FTIR spectra of poly(3-ethyl-3-(hydroxymethyl)oxetanes).

No relationship between the reagents ratio in the POX and peak intensities could be seen, because the FTIR measurements were qualitative. On the other hand, it is clear that respective bands in the spectra of 1:5–1:50 occurred at identical wavenumbers, thus proving great similarity in their structures.

The MALDI-TOF technique allows for a deeper insight into the morphologies and microstructures of polymers. It allows for the confirmation of the mass of repeating unit and the residual mass related to the end group or core molecule. A detailed analysis of the structure of the obtained POXs was performed with this technique. An exemplary MALDI-TOF spectrum is shown in Figure 6. The distance between the a–a (b–b or c–c) peaks was equal to  $116\text{ m/z}$ , which corresponds to a repeating unit of poly(3-ethyl-3-(hydroxymethyl)oxetane). All signals were observed as sodium cation adducts. The most intensive series a can be ascribed to the molecules with the TMP core. The b series  $m/z$  values were lower by 18 and can be ascribed to the macromolecules that contained one cyclic structure T' formed via the dehydration of the terminal T structure and cyclization (Figure 1) [2]. As the reaction was quenched with ethanol, the c series came from POX macromolecule end-capped with ethoxy group. Other signals were in the minority and may have come from products of water elimination.

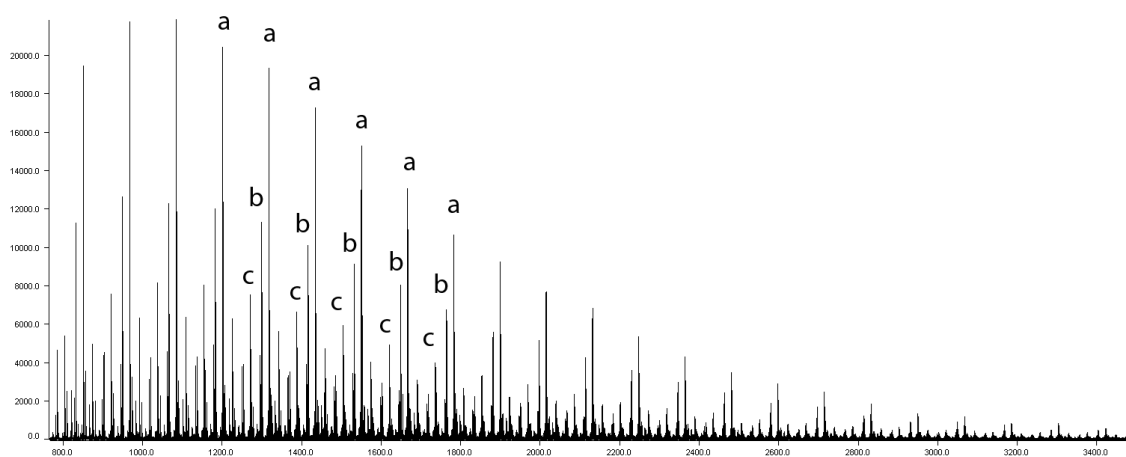


**Figure 6.** MALDI-TOF (DCTB, Na<sup>+</sup>) spectrum of POX with 1,1,1-tris(hydroxymethyl)propane (TMP) core; a-a distance  $\Delta m/z = 116$ .

Theoretical macromolecule weight and size are determined by the amounts and structure of used reagents—the monomer to core ratio. In practice, the statistical nature of polymerization yields a mixture of products of various shapes, branching degrees and molar masses [42]. The molar mass and dispersity of the synthesized polymers are presented in Table 2. One can see that dispersity grew with the growth of the TMP/EHO ratio. This is in agreement with the nature of the ring-opening multibranch polymerization reaction [14,43]. The table does not show a clear relationship between the theoretical and observed values of the number-average ( $M_n$ ) and weight-average ( $M_w$ ) molar mass. This is not surprising because the GPC technique is considered to be error-burden when using polystyrene as the internal standard, because polystyrene's hydrodynamic radius is different from that of the POX. Difficulties in the reliable determination of true average molar mass of hyperbranched polymers by GPC have been described in the literature [44–46].

**Table 2.** Molar mass and dispersity (D) of POXs determined by gel permeation chromatography (GPC).

TMP/EHO Molar Ratio	$M_n$	$M_w$	D
1:5	1240	1690	1.77
1:10	1220	1650	2.18
1:20	1160	1390	2.52
1:50	1310	1850	3.57

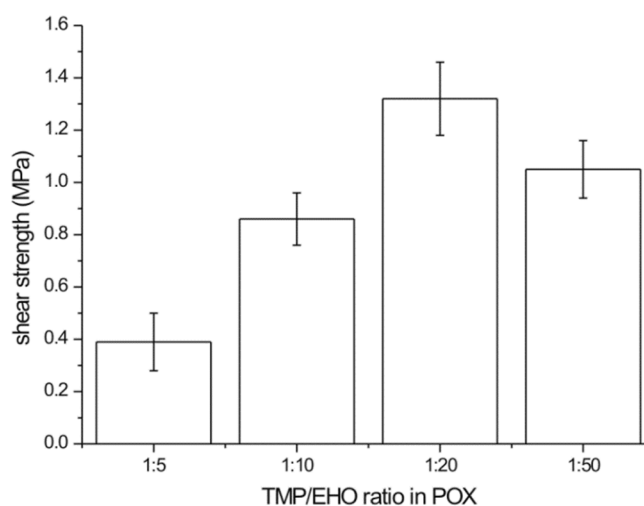
It is commonly agreed that the adhesive interactions of a liquid with a substrate are determined by the surface free energy of the phases, as well as by the interfacial tension between them [36]. It is apparent from Equation (3) that when the interfacial tension,  $\gamma_{SL}$ , is equal to zero, the work of adhesion is maximized. The data in Table 3 indicate that water contact angle ( $\theta$ ) on the POX film (64–67°) was lower than that for the reference commercial hot melt adhesive (82°) and lower than that of polyurethane adhesives (75°) [47], which resulted from the highly polar character of POX due to a high abundance of hydroxyl groups; this low water contact angle demonstrates strong adhesive interactions with polar substrates. The supposition is confirmed by the work of adhesion ( $W_a$ ) values 101–105 mJ/m<sup>2</sup>, which were just ca. 20% lower than the work of adhesion of water on natural wood surfaces (126–133 mJ/m<sup>2</sup>) [36]. Thus, the abovementioned surface characteristics of POXs' films are a sufficient ground to hypothesize that POXs are efficient hot melt adhesives for polar substrate bonding.

**Table 3.** Selected thermal and surface properties of the studied POXs.

TMP/EHO Molar Ratio	$T_s$ [°C]	$T_f$ [°C]	$\theta$ [deg]	$W_a$ [mJ/m <sup>2</sup> ]
1:5	88	105.1	67.2 ± 4.6	101.3 ± 7.2
1:10	87	105.4	66.5 ± 0.6	102.2 ± 0.7
1:20	88	105.2	64.1 ± 2.9	104.5 ± 3.5
1:50	80	105.1	65.4 ± 1.0	104.8 ± 0.4
Reference <sup>a</sup>	–	–	82.1 ± 4.4	80.3 ± 3.5

<sup>a</sup> commercial hot melt;  $T_s$ —softening point;  $T_f$ —flow point;  $\theta$ —water contact angle;  $W_a$ —work of adhesion.

In order to empirically verify the hypothesis, the softening and flow points of the polymers were determined (Table 3). The  $T_s$  values were comparable to those of the commercial hot melt adhesives (88–105 °C) used in furniture manufacturing. Bonding experiments performed on birch veneers revealed apparent differences in joints shear strength (Figure 7). One can see that the POX 1:20 and 1:50 series exhibited much higher values (1.32 MPa and 1.05 MPa, respectively) than those of the 1:5 and 1:10 series (0.39 MPa and 0.86 MPa, respectively). The phenomenon is associated with both the abundance of hydroxyl groups and the ability of hydrogen bond formation, which increases with the degree of branching as well as with the mechanical properties of POXs. Neither of them exhibited cohesive failures in wood, whereas cohesive failure in the POX layer was found in each case (Figure 8). Such behavior resulted from an adhesion to polar substrate that was higher than the cohesion within POXs. As shown in Figure 9, in all cases, a brittle fracture occurred at a low extension during the shear test (0.18–0.97 mm). It is known from the literature that brittle materials fracture under relatively low stress [48], and, moreover, the performance of high modulus adhesives on low modulus substrates is not optimal [49]. However, the brittle character of the investigated POXs cannot be associated with a highly crystalline structure since Mai et al. demonstrated that the degree of crystallinity decreases with increasing degree of branching in POX and is close to 0% for the degree of branching ca. 40% [11]. The highest extension to fracture was observed for the 1:20 POX, which indicates its abilities for higher deformation and stress dissipation than the other investigated POXs. Subsequently, the increased shear strength of the bond-line was yielded.

**Figure 7.** Shear strengths of the POX bond-lines.



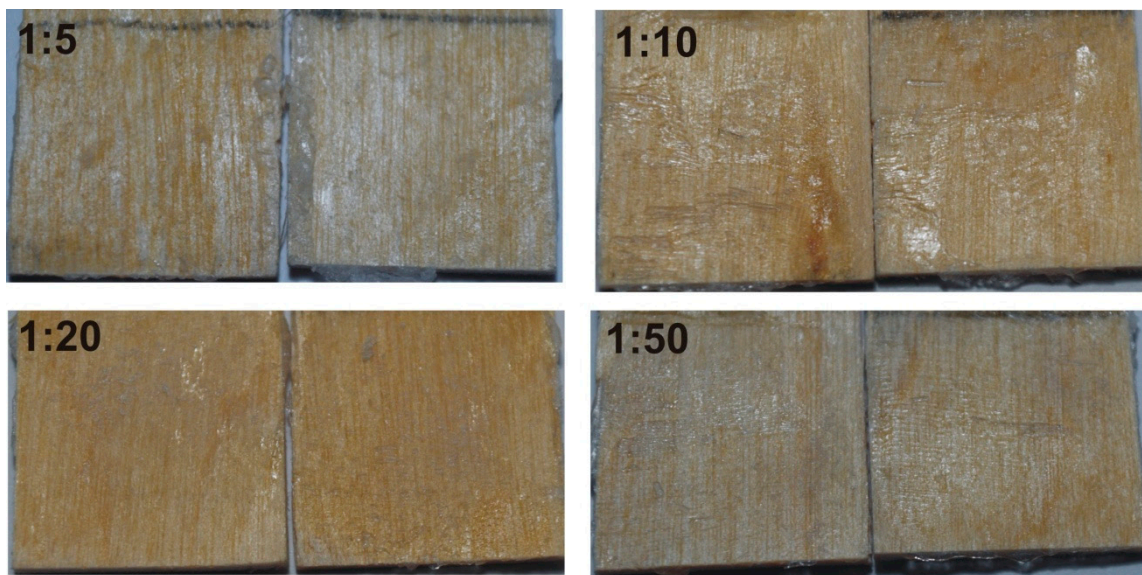


**Figure 8.** Cohesive fracture in POXs layers of different TMP/EHO (3-ethyl-3-(hydroxymethyl)oxetane) ratios.

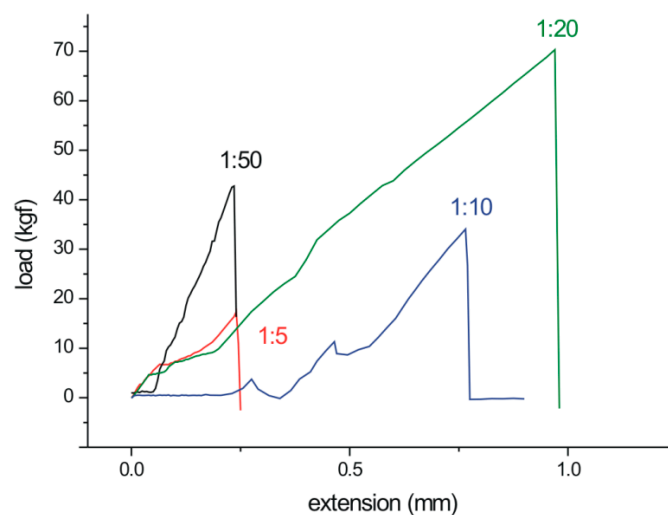


**Figure 9.** The effect of the reagent ratio in the POX molecule on load bearing ability.

The mechanical properties of the bond-lines confirmed our assumptions regarding the strong adhesive interactions of POXs with polar substrates. It is noteworthy that the observed shear strength of the 1:20 series exceeded the minimum required for plywood ( $\geq 1.0$  MPa) [50] and were comparable to those reported for poly(lactide)-poly( $\epsilon$ -caprolactone)-based and ethylene-vinyl acetate based hot-melt adhesives (0.6–1.5 MPa [51]) but still lower than those reported for  $\text{FeCl}_3$ -curable polyoxetanes [30]. Bekhta and Sedliačik investigated plywood bonding with HDPE and demonstrated that shear strengths of the bond-lines greatly depended on the time, pressure, and temperature of the process [52]. The authors obtained the highest strengths for a 160 °C temperature and a 3 min press time, which were necessary for proper penetration of the molten adhesive into the substrate. Similar observations were made by Kajaks and co-workers for polypropylene-based hot-melts [53]. As it is commonly agreed that the quality of bonding strongly depends on processing parameters such as temperature, time and pressure [54], further studies on POX bonding parameters are required. Keeping in mind that the optimization of bonding quality was not the objective of this study, it is likely that a prolonged pressing time and increased temperature would result in the improved strengths of bond-lines.

Thus, the studied POX-based adhesives seem plausible to be used where high mechanical properties of adhesives are not required, e.g., packaging or veneering applications.

However, these findings also indicate that further research should be aimed at the detailed characterization of the thermal, rheological and mechanical properties of POXs, as well as their enhancement via grafting, filling or blending, so that an improved mechanical performance and stress dissipation ability can be incorporated into polymers.

#### 4. Conclusions

Hyperbranched poly(hydroxyl)oxetanes (POXs) were synthesized from 1,1,1-tris(hydroxymethyl)propane (TMP) as a core molecule and 3-ethyl-3-(hydroxymethyl)oxetane (EHO) as a branching monomer. Their hyperbranched structure and chain morphology were confirmed in NMR and MALDI-TOF experiments. It was shown that dispersity grows with the growth of the TMP/EHO ratio, which remains in agreement with the nature of the ring-opening multibranch polymerization reaction. The thermoplastic character of the polymers predisposes them to be potential hot melt adhesives. An analysis of POXs behavior in contact with polar materials proved: (1) strong interactions with polar substrates and high work of adhesion; (2) adhesive interactions with wood that were higher than cohesion within the polymer; (3) the effect of macromolecule structure on the tensile shear strength in the bond-line; and (4) a brittle fracture mode in bond-line.

These findings indicate the need for further investigations on the thermomechanical performance and enhancement of the mechanical properties of poly(hydroxy)oxetanes via chemical modification or doping. Our studies will continue.

**Author Contributions:** Conceptualization, P.P. and M.Ł.M.; methodology, P.P. and M.Ł.M.; synthesis, P.P.; GPC, MALDI-TOF, FTIR and NMR measurements, P.P.; bonding and wetting measurements M.Ł.M.; data analysis, P.P. and M.Ł.M.; writing—Original draft preparation, P.P. and M.Ł.M.; funding acquisition, M.Ł.M. All authors have read and agreed to the published version of the manuscript.

**Funding:** The work was financially supported by The Polish Ministry of Science and Higher Education (grant no. MNiSW/2019/174/DIR)—Innovation Incubator 2.0 program realized at the Warsaw University of Life Sciences—SGGW.

**Acknowledgments:** The authors gratefully thank Olga Kozikowska for help in the experiments.

**Conflicts of Interest:** The authors declare no conflict of interest.

#### References

1. Magnusson, H.; Malmström, E.; Hult, A. Synthesis of hyperbranched aliphatic polyethers via cationic ring-opening polymerization of 3-ethyl-(hydroxymethyl) oxetane. *Macromol. Rapid Commun.* **1999**, *20*, 453–457. [[CrossRef](#)]
2. Bednarek, M.; Biedroń, T.; Heliński, J.; Kałużnyński, K.; Kubisa, P.; Penczek, S. Branched polyether with multiple primary hydroxyl groups: Polymerization of 3-ethyl-3-hydroxymethyloxetane. *Macromol. Rapid Commun.* **1999**, *20*, 369–372. [[CrossRef](#)]
3. Motoi, M.; Nagahara, S.; Akiyama, H.; Horiuchi, M.; Kanoh, S. Preparation of polyoxetane-polystyrene composite resins and their use as polymeric supports of phase-transfer catalysts. *Polym. J.* **1989**, *21*, 987–1001. [[CrossRef](#)]
4. Bednarek, M.; Kubisa, P.; Penczek, S. Multihydroxyl branched polyethers. 2. Mechanistic aspects of cationic polymerization of 3-ethyl-3-(hydroxymethyl) oxetane. *Macromolecules* **2001**, *34*, 5112–5119. [[CrossRef](#)]
5. Yan, D.; Hou, J.; Zhu, X.; Kosman, J.J.; Wu, H.S. A new approach to control crystallinity of resulting polymers: Self-condensing ring opening polymerization. *Macromol. Rapid Commun.* **2000**, *21*, 557–561. [[CrossRef](#)]
6. Mai, Y.; Zhou, Y.; Yan, D.; Lu, H. Effect of reaction temperature on degree of branching in cationic polymerization of 3-ethyl-3-(hydroxymethyl) oxetane. *Macromolecules* **2003**, *36*, 9667–9669. [[CrossRef](#)]
7. Gong, W.; Mai, Y.; Zhou, Y.; Qi, N.; Wang, B.; Yan, D. Effect of the degree of branching on atomic-scale free volume in hyperbranched poly [3-ethyl-3-(hydroxymethyl) oxetane]. A positron study. *Macromolecules* **2005**, *38*, 9644–9649. [[CrossRef](#)]

8. Ye, L.; Gao, P.; Wu, F.; Bai, Y.; Feng, Z.-G. Synthesis and application as polymer electrolyte of hyperbranched copolyethers derived from cationic ring-opening polymerization of 3-[2-[2-(2-methoxyethoxy)ethoxy]ethoxy]methyl- and 3-hydroxymethyl-3'-methyloxetane. *Polymer* **2007**, *48*, 1550–1556. [[CrossRef](#)]
9. Shou, C.; Song, N.; Zhang, Z. Synthesis of hyperbranched poly (3-methyl-3-hydroxymethyloxetane) and their application to separate basic proteins by adsorption coated column. *J. Appl. Polym. Sci.* **2010**, *116*, 2473–2479. [[CrossRef](#)]
10. Rahm, M.; Westlund, R.; Eldsäter, C.; Malmström, E. Tri-block copolymers of polyethylene glycol and hyperbranched poly-3-ethyl-3-(hydroxymethyl)oxetane through cationic ring opening polymerization. *J. Polym. Sci. Part A Polym. Chem.* **2009**, *47*, 6191–6200. [[CrossRef](#)]
11. Mai, Y.; Zhou, Y.; Yan, D.; Hou, J. Quantitative dependence of crystallinity on degree of branching for hyperbranched poly [3-ethyl-3-(hydroxymethyl)oxetane]. *New J. Phys.* **2005**, *7*, 42. [[CrossRef](#)]
12. Chen, Y.; Bednarek, M.; Kubisa, P.; Penczek, S. Synthesis of multihydroxyl branched polyethers by cationic copolymerization of 3,3-bis(hydroxymethyl)oxetane and 3-ethyl-3-(hydroxymethyl)oxetane. *J. Polym. Sci. Part A Polym. Chem.* **2002**, *40*, 1991–2002. [[CrossRef](#)]
13. Bednarek, M.; Kubisa, P. Chain-growth limiting reactions in the cationic polymerization of 3-ethyl-3-hydroxymethyloxetane. *J. Polym. Sci. Part A Polym. Chem.* **2004**, *42*, 245–252. [[CrossRef](#)]
14. Smith, T.J.; Mathias, L.J. Hyperbranched poly (3-ethyl-3-hydroxymethyloxetane) via anionic polymerization. *Polymer* **2002**, *43*, 7275–7278. [[CrossRef](#)]
15. Kudo, H.; Morita, A.; Nishikubo, T. Synthesis of a hetero telechelic hyperbranched polyether. Anionic ring-opening polymerization of 3-ethyl-3-(hydroxymethyl) oxetane using potassium tert-butoxide as an initiator. *Polym. J.* **2003**, *35*, 88–91. [[CrossRef](#)]
16. Morita, A.; Kudo, H.; Nishikubo, T. Synthesis and chemical modification of hyperbranched polyethers with terminal hydroxy groups by the anionic ring-opening polymerization of 3-alkyl-3-hydroxymethyl oxetanes. *J. Polym. Sci. Part A Polym. Chem.* **2004**, *42*, 3739–3750. [[CrossRef](#)]
17. Bednarek, M. Structures and potential applications of multihydroxyl branched polyethers obtained by cationic ring-opening polymerization involving activated monomer mechanism. *e-Polymers* **2008**, *8*, 70. [[CrossRef](#)]
18. del Campo, A.; Bello, A.; Pérez, E. Synthesis of new side-chain liquid-crystalline polyoxetanes with two mesogenic groups connected by a flexible spacer in the side chain. *Macromol. Chem. Phys.* **2002**, *203*, 975–984. [[CrossRef](#)]
19. Sai, R.; Ueno, K.; Fujii, K.; Nakano, Y.; Tsutsumi, H. Steric effect on Li<sup>+</sup> coordination and transport properties in polyoxetane-based polymer electrolytes bearing nitrile groups. *RSC Adv.* **2017**, *7*, 37975–37982. [[CrossRef](#)]
20. Sai, R.; Fujii, K.; Nakano, Y.; Shigaki, N.; Tsutsumi, H. Role of polar side chains in Li<sup>+</sup> coordination and transport properties of polyoxetane-based polymer electrolytes. *Phys. Chem. Chem. Phys.* **2017**, *19*, 5185–5194. [[CrossRef](#)]
21. Zheng, Y.; Wynne, K.J. Poly (bis-2,2,2-trifluoroethoxymethyl oxetane): Enhanced surface hydrophobicity by crystallization and spontaneous asperity formation. *Langmuir* **2007**, *24*, 11964–11967. [[CrossRef](#)] [[PubMed](#)]
22. Gervais, M.; Forens, A.; Ibarboure, E.; Carlotti, S. Anionic polymerization of activated oxetane and its copolymerization with ethylene oxide for the synthesis of amphiphilic block copolymers. *Polym. Chem.* **2018**, *9*, 2660–2668. [[CrossRef](#)]
23. Nair, S.S.; McCullough, E.J.; Yadavalli, V.K.; Wynne, K.J. Integrated compositional and nanomechanical analysis of a polyurethane surface modified with a fluorinated oxetane siliceous-network hybrid. *Langmuir* **2014**, *30*, 12986–12995. [[CrossRef](#)] [[PubMed](#)]
24. Chakrabarty, S.; Wang, C.; Zhang, W.; Wynne, K.J. Rigid adherent-resistant elastomers (RARE): Nano-, meso-, and microscale tuning of hybrid fluorinated polyoxetane–polyurethane blend coatings. *Macromolecules* **2013**, *46*, 984–2996. [[CrossRef](#)]
25. Sharma, K.; Zolotarskaya, O.Y.; Wynne, K.J.; Yang, H. Poly (ethylene glycol)-armed hyperbranched polyoxetanes for anticancer drug delivery. *J. Bioact. Compat. Polym.* **2012**, *27*, 525–539. [[CrossRef](#)]
26. Zolotarskaya, O.Y.; Wagner, A.F.; Beckta, J.M.; Valerie, K.; Wynne, K.J.; Yang, H. Synthesis of water-soluble camptothecin–polyoxetane conjugates via click chemistry. *Mol. Pharm.* **2012**, *9*, 3403–3408. [[CrossRef](#)]
27. Zolotarskaya, O.Y.; Yuan, Q.; Wynne, K.J.; Yang, H. Synthesis and characterization of clickable cyto-compatible poly(ethylene glycol)-grafted polyoxetane brush polymers. *Macromolecules* **2013**, *46*, 63–71. [[CrossRef](#)]

28. Makal, U.; Uilk, J.; Kurt, P.; Cooke, R.S.; Wynne, K.J. Ring opening polymerization of 3-semifluoro- and 3-bromomethyloxetanes to poly (2,2-substituted-1,3-propylene oxide) telechelics for soft blocks in polyurethanes. *Polymer* **2005**, *46*, 2522–2530. [[CrossRef](#)]
29. Kurt, P.; Wynne, K.J. Co-polyoxetanes with alkylammonium and fluorous or PEG-like side chains: Soft blocks for surface modifying polyurethanes. *Macromolecules* **2007**, *40*, 9537–9543. [[CrossRef](#)]
30. Jia, M.; Li, A.; Mu, Y.; Jiang, Y.; Wan, X. Synthesis and adhesive property study of polyoxetanes grafted with catechols via Cu(I)-catalyzed click chemistry. *Polymer* **2014**, *55*, 1160–1166. [[CrossRef](#)]
31. Li, A.; Jia, M.; Mu, Y.; Jiang, W.; Wan, X. Humid bonding with a water-soluble adhesive inspired by mussels and sandcastle worms. *Macromol. Chem. Phys.* **2015**, *216*, 450–459. [[CrossRef](#)]
32. Cho, J.-D.; Han, S.-T.; Hong, J.-W. A novel in situ relative-conductivity-based technique for monitoring the cure process of UV-curable polymers. *Polym. Test.* **2007**, *26*, 71–76. [[CrossRef](#)]
33. Sasaki, H. Photocurable pressure-sensitive adhesives using alkyl oxetane. In *Photoinitiated Polymerization*; Belfield, K.D., Crivello, J.V., Eds.; American Chemical Society: Washington, DC, USA, 2003; Volume 847, pp. 296–305.
34. Mamiński, M.; Wawrzyńska, E.; Parzuchowski, P. Application of Poly (Hydroxy) Oxetanes and Hot-Melt Adhesive for Wood Bonding. Polish Patent Application No. P-417267, 19 May 2016.
35. Penczek, S.; Kubisa, P.; Szymański, R. Activated monomer propagation in cationic polymerizations. *Makromol. Chem. Makromol. Symp.* **1986**, *3*, 203–220. [[CrossRef](#)]
36. Wolkenhauer, A.; Avramidis, G.; Hauswald, E.; Militz, H.; Viöl, W. Sanding vs. plasma treatment of aged wood: A comparison with respect to surface energy. *Int. J. Adhes. Adhes.* **2009**, *29*, 18–22. [[CrossRef](#)]
37. Gindl, M.; Sinn, G.; Gindl, W.; Reiterer, A.; Tschegg, S. A comparison of different methods to calculate the surface free energy of wood using contact angle measurements. *Colloids Surf A Physicochem. Eng. Asp.* **2001**, *181*, 279–287. [[CrossRef](#)]
38. Kubisa, P.; Penczek, S. Cationic activated monomer polymerizations of heterocyclic monomers. *Prog. Polym. Sci.* **1999**, *24*, 1409–1437. [[CrossRef](#)]
39. Bednarek, M.; Kubisa, P. Application of poly (3-ethyl-3-hydroxymethyloxetane) as macroinitiator for the synthesis of star polymers of ethylene oxide. Efficiency of initiation. *Polimery* **2004**, *49*, 719–723. [[CrossRef](#)]
40. Haag, R.; Stumbe, J.-F.; Sunder, A.; Frey, H.; Hebel, A. An approach to core shell-type architectures in hyperbranched polyglycerols by selective chemical differentiation. *Macromolecules* **2000**, *33*, 8158–8166. [[CrossRef](#)]
41. Mamiński, M.; Parzuchowski, P.; Trojanowska, A.; Dziewulski, S. Fast-curing polyurethane adhesives derived from environmentally friendly hyperbranched polyglycerols—The effect of macromonomer structure. *Biomass Bioenergy* **2011**, *35*, 4446–4468. [[CrossRef](#)]
42. Hölter, D.; Burgath, A.; Frey, H. Degree of branching in hyperbranched polymers. *Acta Polym.* **1997**, *48*, 30–35. [[CrossRef](#)]
43. Galina, H.; Krawczyk, M. A simple model of hyperbranched polymerisation involving AB<sub>2</sub> and B<sub>f</sub> core monomers and methods of narrowing the molecular size distribution. *Polym. Bull.* **2007**, *58*, 83–91. [[CrossRef](#)]
44. Kim, Y. Hyperbranched polymers 10 years after. *J. Polym. Sci. Part A Polym. Chem.* **1998**, *36*, 1685–1698. [[CrossRef](#)]
45. Sunder, A.; Hanselmann, R.; Frey, H.; Mühlaupt, R. Controlled synthesis of hyperbranched polyglycerols by ring-opening multibranching polymerization. *Macromolecules* **1999**, *32*, 4240–4246. [[CrossRef](#)]
46. Rokicki, G.; Rakoczy, P.; Parzuchowski, P.; Sobiecki, M. Hyperbranched aliphatic polyethers obtained from environmentally benign monomer: Glycerol carbonate. *Green Chem.* **2005**, *7*, 529–539. [[CrossRef](#)]
47. Bahattab, M.A.; Donate-Robles, J.; García-Pacios, V.; Martín-Martínez, J.M. Characterization of polyurethane adhesives containing nanosilicas of different particle size. *Int. J. Adhes. Adhes.* **2011**, *31*, 97–103. [[CrossRef](#)]
48. Suo, Z. Failure of brittle adhesive joints. *Appl. Mech. Rev.* **1990**, *43*, 276–279. [[CrossRef](#)]
49. Gordon, T.L.; Fakley, M.E. The influence of elastic modulus on adhesion to thermoplastics and thermoset materials. *Int. J. Adhes. Adhes.* **2003**, *23*, 95–100. [[CrossRef](#)]
50. EN 314-2. *Plywood—Bonding Quality—Part 2: Requirements*; European Committee for Standardization (CEN): Brussels, Belgium, 1993.
51. Viljanmaa, M.; Södergård, A.; Törmälä, P. Lactic acid based polymers as hot melt adhesives for packaging applications. *Int. J. Adhes. Adhes.* **2002**, *22*, 219–226. [[CrossRef](#)]

52. Bekhta, P.; Sedliačik, J. Environmentally-friendly high-density polyethylene-bonded plywood panels. *Polymers* **2019**, *11*, 1166. [[CrossRef](#)]
53. Kajaks, J.A.; Bakradze, G.G.; Viksne, A.V.; Reihmane, S.A.; Kalnins, M.M.; Krutohvastov, R. The use of polyolefins-based hot melts for wood binding. *Mech. Compos. Mater.* **2009**, *45*, 643–650. [[CrossRef](#)]
54. Smith, M.J.; Dai, H.; Ramani, K. Wood-thermoplastic adhesive interface—Method of characterization and results. *Int. J. Adhes. Adhes.* **2002**, *22*, 197–204. [[CrossRef](#)]



© 2020 by the authors. Licensee MDPI, Basel, Switzerland. This article is an open access article distributed under the terms and conditions of the Creative Commons Attribution (CC BY) license (<http://creativecommons.org/licenses/by/4.0/>).